

Organization and Adhesive Properties of the Hyaluronan Pericellular Coat of Chondrocytes and Epithelial Cells

Miriam Cohen,^{*‡} Eugenia Klein,[†] Benjamin Geiger,^{*} and Lia Addadi[‡]

^{*}Department of Molecular Cell Biology, [†]Chemical Research Services Unit, and [‡]Department of Structural Biology, Weizmann Institute of Science, Rehovot 76100, Israel

ABSTRACT Hyaluronan is a megadalton glycosaminoglycan composed of repeating units of *D-N*-acetylglucosamine- β -*D*-Glucuronic acid. It is known to form a highly hydrated pericellular coat around chondrocytes, fibrosarcoma, and smooth muscle cells. Using environmental scanning electron microscopy we detected fully hydrated hyaluronan pericellular coats around rat chondrocytes (RCJ-P) and epithelial cells (A6). Hyaluronan mediates early adhesion of both chondrocytes and A6 cells to glass surfaces. We show that chondrocytes in suspension establish early “soft contacts” with the substrate through a thick, hyaluronidase-sensitive coat ($4.4 \pm 0.7 \mu\text{m}$). Freshly-attached cells drift under shear stress, leaving hyaluronan “footprints” on the surface. This suggests that chondrocytes are surrounded by a multilayer of entangled hyaluronan molecules. In contrast, A6 cells have a $2.2 \pm 0.4 \mu\text{m}$ -thick hyaluronidase-sensitive coat, do not drift under shear stress, and remain firmly anchored to the surface. We consider the possibility that in A6 cells single hyaluronan molecules, spanning the whole thickness of the pericellular coat, mediate these tight contacts.

INTRODUCTION

Cell adhesion to the extracellular matrix (ECM) is a complex multicomponent process, which is involved in the regulation of cell motility, proliferation, differentiation, and survival. Cell-ECM contact commonly occurs at specialized sites such as focal adhesions where the interaction is mediated via heterodimeric transmembrane adhesion receptors of the integrin family (Geiger et al., 2001; Martin et al., 2002). These molecules are directly associated, through their extracellular domains, with specific ECM networks, and link them to the actin cytoskeleton (Adams, 2001; Geiger et al., 2001). The transmembrane interactions of integrins with F-actin are mediated by complex networks of plaque proteins that regulate both the assembly and stability of the contacts, and the signaling processes.

Matrix adhesion is a multistage process, involving, in addition to the integrin-mediated adhesion, an integrin-independent cell-ECM interaction (Hanein et al., 1993, 1994, 1995; Zimmerman et al., 2002). Using a variety of adhesive surfaces, it was shown that the early stages of attachment of A6 cells (epithelial cells of *Xenopus laevis*) are resistant to inhibition by RGD, the integrin-specific peptide, and to cytoskeleton-disrupting drugs (Hanein et al., 1993, 1994). This early adhesion was shown to occur at a timescale of seconds, and to be mediated by cell-surface hyaluronan (Zimmerman et al., 2002).

Hyaluronan is a large linear glycosaminoglycan, with typical molecular mass of a few million Daltons (Toole, 2001), composed of a repeating disaccharide of [*D-N*-acetylglucosamine- β -*D*-Glucuronic acid] (Lee and Spicer, 2000). Due

to the carboxyl group of the glucuronic acid, hyaluronan is highly negatively charged at physiological pH, and behaves in solution as a polyelectrolyte, forming a viscous gel. Dry, surface-grafted hyaluronan layers can swell within a few seconds, adsorbing water to 2.4-fold their initial thickness (Mathe et al., 1999). The ability to adsorb large amounts of water, combined with the repulsion between identically charged groups, makes hyaluronan a good lubricant (Israelachvili and Wennerstrom, 1996; Tadmor et al., 2002).

Hyaluronan can either be secreted by the cells to the ECM or associated with the plasma membrane. As an ECM component hyaluronan is involved in mediating and modulating cell adhesion as well as in maintaining osmotic balance and reducing friction in tissues such as the synovium, vitreous humor, and cartilage (Toole, 2001). At the cell surface it is known to comprise a pericellular coat, which can be visualized as a hyaluronidase-sensitive area in particle-exclusion assays. Due to intrinsic limitations of this approach only substantial coats can be detected, such as in fibrosarcoma cells (McBride and Bard, 1979), chondrocytes (Lee et al., 1993), and smooth muscle cells (Evanko et al., 1999).

The adhesion of A6 cells to the substrate was shown to be drastically attenuated when the cells are treated with hyaluronidase, which hydrolyzes hyaluronan by randomly cleaving the β -*N*-acetyl-glucosamine-[1-4] glycosidic bonds (Zimmerman et al., 2002). Addition of exogenous hyaluronan to the treated cells or to the substrate restores cell adhesion, whereas addition of hyaluronan to both the cells and the surface inhibits the adhesion (Zimmerman et al., 2002). This indicates that hyaluronan can enhance or block cell adhesion, depending on whether it is present on the cell surface, on the substrate, or on both.

To understand the mechanism of ECM adhesion mediated by cell-surface hyaluronan, it is important to establish the physical properties, including the thickness, of this layer. The major difficulty in visualizing a hyaluronan layer arises

Submitted January 14, 2003, and accepted for publication April 2, 2003.

Address reprint requests to Lia Addadi, Dept. of Structural Biology, Weizmann Institute of Science, Rehovot 76100, Israel. Tel.: 972-8-9344105; Fax: 972-8-9344151; E-mail: lia.addadi@weizmann.ac.il.

© 2003 by the Biophysical Society

0006-3495/03/09/1996/10 \$2.00

from its highly hydrated nature. Dehydration of such samples, a mandatory step in conventional (non cryo-) electron microscopy techniques, generates a distorted view of cell surfaces, inevitably reducing a hydrated pericellular coat to dispersed fibers. Indeed, the substantial pericellular coat of human smooth muscle cells (Evanko et al., 1999), or of fibrosarcoma cells, appears as a sparse fibrous matrix after air-drying or freeze-drying, respectively (Bard et al., 1983).

Hyaluronan molecules are being simultaneously synthesized and extruded through the cell membrane by a transmembranal glycosyltransferase, hyaluronan synthase. A portion of these hyaluronan molecules remains anchored to the hyaluronan synthase (Weigel et al., 1997), whereas the rest are released from the cells and bind either to integral membrane hyaluronan receptors, mainly CD44 (Bajorath, 2000), or to the ECM. It is not clear whether hyaluronan molecules are attached to receptors on the membrane to form a “de Gennes brush configuration” (de Gennes, 1987; Lee et al., 1993; Toole, 2001), or rather form multilayered gels where nonanchored hyaluronan molecules are entangled with the receptor-grafted molecules.

The striking observation of hyaluronan-mediated adhesion of A6 cells to various surfaces (Hanein et al., 1993, 1994, 1995; Zimmerman et al., 2002) raises the question of the generality of this phenomenon to other cell types and of the ability of a thick hyaluronan pericellular coat, such as that surrounding chondrocytes, to mediate cell-substrate adhesion (Lee et al., 1993).

In this study we visualized the cell-bound hyaluronan of RCJ-P rat chondrocytes and A6 *Xenopus* epithelial cells, using an environmental scanning electron microscope (ESEM) (Danilatos, 1991) and a particle exclusion assay based on 3D reconstruction from fluorescence microscopy. This examination revealed a thick coat around both cells. We further found that the initial adhesion of rat chondrocytes to glass surfaces is hyaluronan mediated, as is that of A6 cells. The mechanical properties of these early cell adhesions suggest that, whereas in chondrocytes hyaluronan forms thick entangled multilayers, in A6 cells the interaction is mediated by hyaluronan molecules attached directly to the membrane.

MATERIALS AND METHODS

Cell culture

RCJ-P chondrocytes (rat chondrocytes from fetal calvaria, batch 15.01.98; Prochon Biotech, Rehovot, Israel) were cultured at 37°C in humidified atmosphere of 5% CO₂ in air in α -minimum essential medium (Biological Services, The Weizmann Institute) supplemented with 15% fetal calf serum (Biolab Ltd., Jerusalem, Israel).

A6 cells (kidney epithelial cells from *Xenopus laevis*, ATCC.CCL 102) were cultured at 27°C in humidified atmosphere of 5% CO₂ in air in Dulbecco's minimum essential medium (Biological Services, The Weizmann Institute) diluted to 85% with water and supplemented with 10% fetal calf serum (Biolab Ltd.).

Glass coverslips, used for cell culturing, were coated with serum by incubation for 3–16 h with 10% fetal calf serum (Biolab Ltd.).

Cell treatment with hyaluronidase

Cells were suspended using trypsin-EDTA (Biological Services, The Weizmann Institute), centrifuged, and resuspended in serum-free medium. Hyaluronidase (hyaluronidase type IV-S from bovine testes, Sigma, St. Louis, MO) was added to the suspended cells to a final concentration of 500 units/ml. Incubation was performed at 37°C for RCJ-P cells. A6 cells were incubated at 37°C for the flow experiments and at 27°C for the ESEM experiments. After treatment, the cells were centrifuged, and washed three times with serum-containing medium to remove residual enzyme and hyaluronan fragments. Cells were then resuspended in serum-containing medium.

Sample preparation for conventional (dry) scanning electron microscopy

Cells were suspended using trypsin-EDTA, centrifuged, and gently resuspended in serum-containing medium. They were then seeded on glass coverslips and incubated for 25 min at 37°C (RCJ-P) or 10 min at 27°C (A6). Fixation was performed with 2% glutaraldehyde in 0.1 M cacodylate buffer, 5 mM CaCl₂, pH 7.2, for 30 min, followed by three rinses (5 min each) with 0.1 M cacodylate buffer. The cells were postfixated for 1 h with 1% osmium tetroxide in the same buffer. The coverslips were then rinsed, dehydrated with ethanol, and critical point dried with CO₂ (Pelco CPD2, Ted Pella, Redding, CA). The samples were sputter-coated with thin film of the order of 10 nm of gold-palladium (S 150, BOC Edwards, Sussex, UK) and examined in the environmental scanning electron microscope, XL 30 ESEM FEG (Philips/FEI, Eindhoven, Netherlands) operated at 10 kV using high vacuum mode.

Preparation of hydrated sample for environmental scanning electron microscopy

Suspended cells were centrifuged, washed, and fixed with 2% glutaraldehyde in 0.1 M cacodylate buffer, 5 mM CaCl₂, pH 7.2, for 30 min. After rinsing with 0.1 M cacodylate buffer for 5 min, and three times with water (5 min each), the cells were incubated for 45 min with 2% uranyl acetate in water at pH 3.5, washed, resuspended in water, and seeded on serum-coated glass coverslips at 4°C for 16 h. For osmium tetroxide labeling, the fixed cells were rinsed with 0.1 M cacodylate buffer instead of water, and incubated for 45 min with 1% osmium tetroxide in the same buffer. Finally the cells were washed twice with water and seeded on serum-coated coverslips. The samples were examined in the environmental scanning electron microscope, XL 30 ESEM FEG (Philips/FEI) at 10 kV, using wet mode at 5°C, 6.4 Torr (867 Pascal), 7.8 mm working distance.

Particle exclusion assay

Suspended RCJ-P cells were centrifuged, washed, and resuspended in serum-containing medium. They were then seeded in 35-mm tissue culture plates on serum-coated coverslips and incubated for 25 min at 37°C. The cells were washed and fixed with 2% glutaraldehyde in 0.1 M cacodylate buffer, 5 mM CaCl₂, pH 7.2, for 30 min. They were then rinsed with 0.1 M cacodylate buffer for 5 min, and three times with water for 5 min each. The cells were stained with CY3 reactive dye (#Q13008, Biological Detection Systems, Pittsburgh, PA) in PBS for 3 min, and washed with water to remove excess dye. FITC-labeled 0.4- μ m silica beads (kindly provided by Prof. S. Margel, Bar Ilan University, Ramat Gan, Israel) were added to the plate so that the cells were completely immersed in beads. Micrographs were taken with a digital microscope system (DeltaVision, Applied Precision, Inc., Issaquah, WA) as previously described (Zamir et al., 1999). Image acquisition and processing were performed with Resolve3D and Priism programs (Zamir et al., 1999).

For 3D imaging, a series of z-sections were taken at 0.5- μ m intervals. The images were reconstructed with the full deconvolution-based imaging of the Priism software.

Cells under shear flow

Suspended RCJ-P cells were centrifuged, washed, and resuspended in serum-containing medium. They were seeded on 35-mm serum-coated glass coverslips (Marienfeld, Bad Mergentheim, Germany), and incubated for 25 min at 37°C. The cells were then placed in a parallel plate flow chamber (GlycoTech, Rockville, MD) at 37°C, and subjected to flow, exerting a shear stress of 6.5 dyne/cm², applied for three minutes by peristaltic pump (Minipuls3, Gilson, Middleton, WI). Time-lapse movies were taken with DeltaVision digital microscope at 2-s intervals.

A6 cells were treated in the same manner, except that uncoated glass coverslips (batch by special order Marienfeld, Bad Mergentheim, Germany) were used. Cells were incubated for 5 min at 27°C before application of the flow.

Hyaluronan “footprint” labeling

Cells were exposed to flow for 3 min, as described above, then fixed for 20 min with 3% paraformaldehyde in phosphate-buffered saline (PBS) (Biological Services, The Weizmann Institute). The cells were washed three times with PBS, 10 min each, then incubated for 2 h at 37°C with 1:100 biotinylated hyaluronic acid binding protein (bHABP, 0.5 mg/ml, Seikagaku, Japan). They were then washed three times with PBS, for 15 min each, incubated with 1:200 CY3-conjugated streptavidin (1.8 mg/ml, ENCO, Petach Tiqva, Israel) for 30 min at 37°C, and washed again. Micrographs were taken with the DeltaVision digital microscope.

RESULTS

Visualization of cell-associated hyaluronan layers using the ESEM

The introduction of the ESEM has revolutionized the observation of biological samples by scanning electron microscopy by enabling direct examination of biological specimens in an aqueous environment. The microscope is designed to operate in atmosphere containing water at a pressure of up to 10 Torr (1333 Pascal). Thus, samples can be imaged in a humid environment in equilibrium with liquid H₂O and/or with water vapor. These features are particularly critical for examination of hydrated gels, which undergo radical and irreversible changes upon dehydration. Our primary reference cells for studying the pericellular coat by ESEM were chondrocytes (RCJ-P) whose pericellular coat was reported to be in the range of several μm thick (Lee et al., 1993). Various approaches were undertaken to visualize the pericellular coat, including conventional fixation with glutaraldehyde followed by treatment with osmium tetroxide. All these treatments failed to reveal cell-associated material outside the plasma membrane (see below). Finally, treatment with uranyl acetate was attempted, with the idea that the heavy uranyl ions UO_2^{2+} would bind to the negatively charged hyaluronan and concomitantly favor its visualization. Indeed, examination of fixed RCJ-P cells deposited on glass coverslips from suspension and incubated with 2% uranyl acetate at pH 3.5 revealed a $4.4 \pm 0.7\text{-}\mu\text{m}$ -wide, sharply defined halo around the cells (Fig. 1 *a*). A6 epithelial cells subjected to the same treatment were surrounded by a $2.2 \pm 0.4\text{-}\mu\text{m}$ -thick halo (Fig. 1 *b*).

Both RCJ-P and A6 cells treated with hyaluronidase to remove cell-bound hyaluronan (before fixation) and then incubated with uranyl acetate, did not display a halo when examined with ESEM (Fig. 1, *c* and *d*), supporting the notion that this halo indeed represents a hyaluronan-based pericellular coat.

The hyaluronan coat alone (i.e., without staining with uranyl acetate) is completely transparent to the electron beam, and thus no halo is visible around unstained cells (Fig. 1, *e* and *f*). The uranyl-labeled hyaluronan halo appears, however, to be semitransparent to electrons; the image of the cell membrane obtained through the labeled coat appears uniformly blurred, although the depth of field is well above the cell thickness (Fig. 1, *a* and *b*). In contrast, hyaluronidase-treated cells and cells that were not incubated with uranyl acetate display sharp borders (Fig. 1, *c-f*).

Critical point drying of RCJ-P cells results in the disappearance of the hyaluronan gel from the cell surface and exposure of the underlying microvilli (Fig. 1 *g*). The surface texture of A6 cells is quite different, being dominated by broad lamellae and membrane folds (Fig. 1 *h*). As expected, the surface-bound gel is not retained upon dehydration.

The ESEM also makes it possible to monitor the dehydration of the hyaluronan coat upon reduction of pressure in the ESEM chamber (Fig. 2). Chondrocytes (RCJ-P) were fixed and labeled with 2% uranyl acetate, pH 5.0, as described above, and examined by the ESEM (Fig. 2 *a*). Gradual reduction in pressure resulted in slow evaporation of the gel-retained water and, consequently, dehydration of the gel (Fig. 2 *b*). The dehydration resulted in shrinkage of the cells to 80% of their original projected area, and disappearance of the gel. Traces of uranyl acetate remain associated with the matrix at pH 5.0, thus marking the area that was associated with hyaluronan before dehydration (see below) (Fig. 2 *b*).

Binding of uranyl ions to the hyaluronan coat of chondrocytes is highly pH-dependent. Cells incubated with uranyl acetate at pH 3.1 (Fig. 3 *a*) or at pH 4.3 (Fig. 3 *c*) were positively labeled, but the signal was not as strong as at pH 3.5 (Fig. 3 *b*). At pH 5.0 uranyl acetate stains the hyaluronan gel, but tends to precipitate within the fixed gel because of reduced solubility (Fig. 3 *d*). Chondrocytes were also incubated with uranyl acetate oxalate at pH 7.0, the rationale being that at this pH hyaluronan should be fully negatively charged and thus maximally bind the uranyl cations. No staining of the gel was detected under these conditions, however (Fig. 3 *e*), probably because the solubility of uranyl acetate at this pH is too low.

The standard procedure for preparing samples for scanning electron microscopy includes postfixation with osmium tetroxide (OsO_4), which particularly binds to lipids in the cell membrane. Such fixation enhanced the contour of the cell body, but did not highlight the cell-bound hyaluronan gel (Fig. 3 *f*).

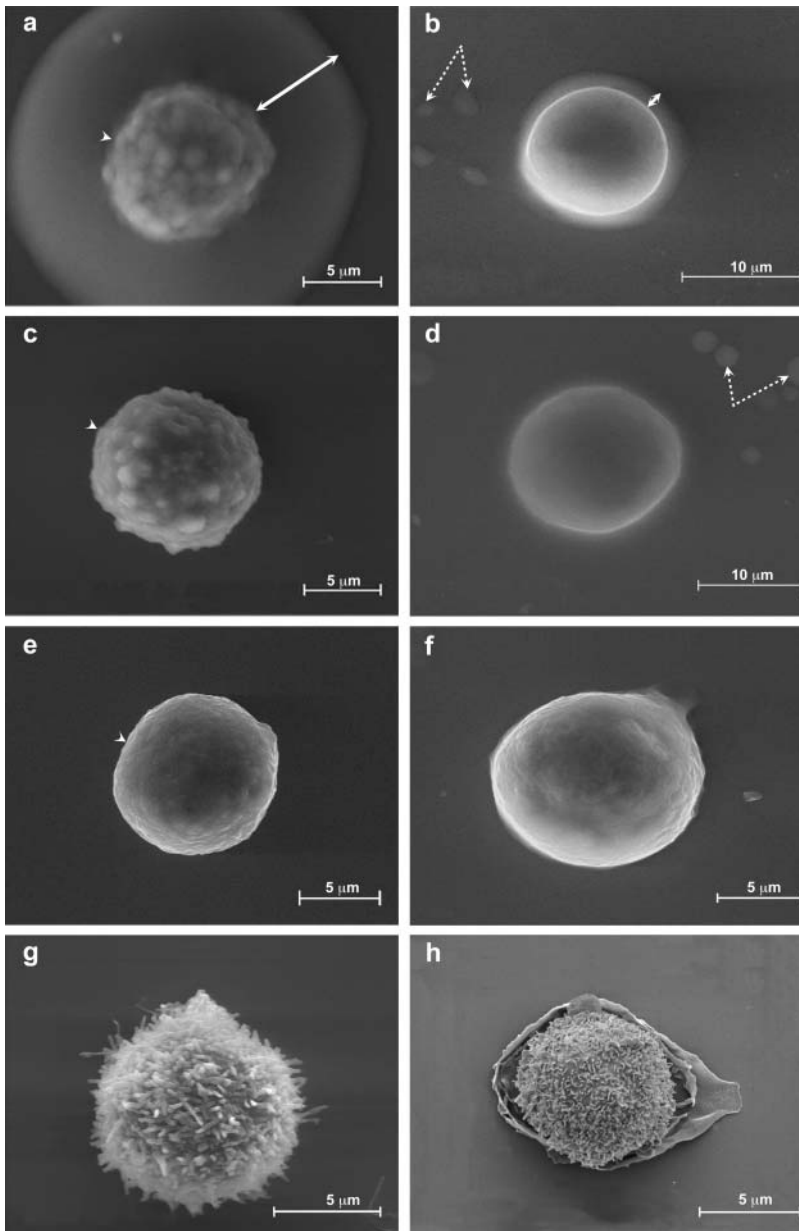


FIGURE 1 Visualization of hydrated pericellular coats using the environmental scanning electron microscope. Chondrocytes (RCJ-P: *a, c, e, g*) and epithelial cells (A6: *b, d, f, h*) examined in the ESEM. (*a* and *b*) Untreated cells, labeled with uranyl ions; (*c* and *d*) hyaluronidase-treated cells; (*e* and *f*) untreated cells, not labeled with uranyl ions; (*g* and *h*) critical point dried cells. The cells were labeled with uranyl acetate at pH 3.5 after fixation; the uranyl ions bind to hyaluronan, resulting in visualization of a 4.4 ± 0.7 - μm -thick halo around RCJ-P cells (*a*) and a 2.2 ± 0.4 - μm -thick halo around A6 cells (*b*). Arrows indicate the gel, dashed arrows indicate water droplets in equilibrium with the wet environment. The cell membrane looks blurred through the gel (*a*, arrowhead). Hyaluronidase-treated cells are not surrounded by halos, and their borders are well defined (*c, d*, arrowhead). In cells that were not incubated with uranyl acetate (*e* and *f*) and in critical point dried cells (*e* and *f*), no gel is detected.

3D visualization of the pericellular hyaluronan coat of chondrocytes by particle exclusion assay

The ESEM images of fixed chondrocytes (RCJ-P) and epithelial cells (A6) directly deposited from suspension showed that these cells are surrounded by a several- μm -thick layer of hyaluronan. ESEM cannot, however, provide direct information on the thickness of the coat in the vertical dimension, on the apical cell surface. In other words, the cells may be entirely coated by hyaluronan or, alternatively, the hyaluronan coat may have “oozed” from the cell surface to the nearby glass surface, at least in part. To better evaluate the thickness of the coat in the vertical dimension, a particle exclusion assay based on fluorescence was employed. Chondrocytes were allowed to adhere to glass coverslips

for 25 min before fixation under the same conditions used for the ESEM. The cells were then directly labeled with tetramethyl rhodamine iso-thiocyanate (red). After gentle washing, the cells were incubated with a large excess of FITC-labeled 0.4- μm silica beads (green), such that they were completely immersed in beads, yet the beads would be excluded from the viscous zone of pericellular gel. Serial optical sections 0.5 μm apart in depth were recorded using the digital DeltaVision microscope, which can generate 3D images by deconvolution-based 3D image reconstruction. A top view of such sections confirms that a 5- to 6- μm zone from which beads are excluded surrounds untreated chondrocytes (dark area in Fig. 4 *a* and Movie 1 *a*, Supplementary Material), whereas the beads can access the surface of

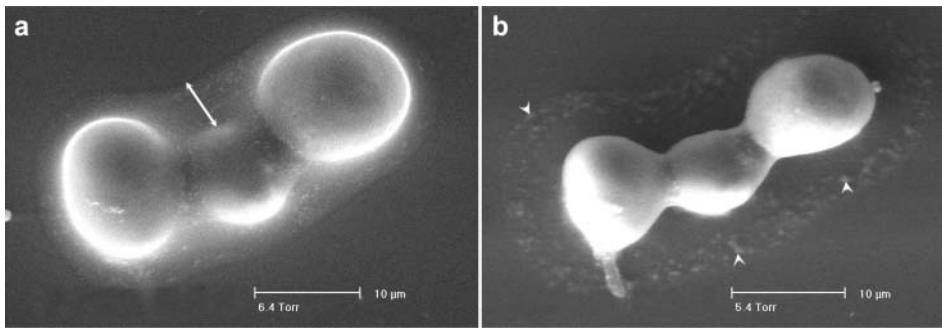


FIGURE 2 The hyaluronan coat disappears upon dehydration. Chondrocytes were labeled with uranyl acetate, pH 5.0, after fixation and examined in the ESEM. (a) At 6.4 Torr (853 Pascal), the dew point, the pericellular coat is visible around the cells (arrow). (b) Gradual reduction of the pressure to 5.4 Torr (720 Pascal) resulted in dehydration and disappearance of the gel. Arrowheads indicate residual traces of uranyl acetate.

hyaluronidase treated cells (Fig. 4 *b* and Movie 1 *b*, Supplementary Material). The deconvoluted and reconstructed image shows an exclusion area, 1.2 μm thick, above the cells (Fig. 4 *c* and Movie 1 *c*, Supplementary Material; see figure legend for further technical details). Again, hyaluronidase-treated cells have no excluded volume around them (Fig. 4 *d* and Movie 1 *d*, Supplementary Material). These data confirm that the hyaluronan coat indeed surrounds the entire cell, including the apical aspect, where its thickness is $>1 \mu\text{m}$. The reduced thickness of the gel in the upper part of the cell may be due to the 25-min incubation of the cells before observation, which allows them to undergo at least partial spreading. It was unfortunately impossible to visualize cells directly deposited from suspension, because they are not well anchored on the glass, thus preventing imaging of a z-series.

The role of the hyaluronan coat in regulating the mechanical properties of early adhesions of chondrocytes

We have previously demonstrated that hyaluronan mediates and modulates matrix adhesion of A6 epithelial cells to a variety of surfaces (Zimmerman et al., 2002). To assess whether early adhesion of chondrocytes is also hyaluronan mediated, and to test the mechanical properties of the hyaluronan-mediated early cell adhesions, suspended RCJ-P cells were allowed to adhere for 25 min to serum-coated glass (Fig. 5 *c*). The cells were then subjected to a continuous flow of medium, which applies to them a constant shear force of 6.5 dyne/cm^2 . Cells before and during the application of force were recorded by time-lapse video microscopy (Fig. 5 *d* and Movie 2 *a*, Supplementary Material). Comparison of the number of untreated cells before and after application of

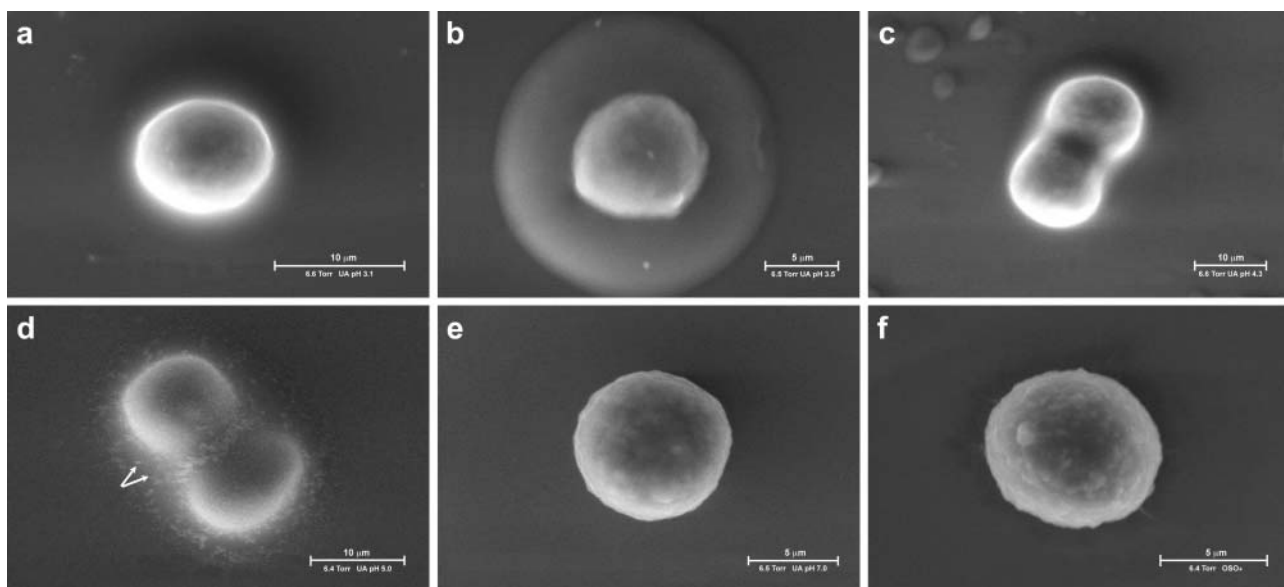


FIGURE 3 The mode of binding uranyl ions to the hyaluronan coat of chondrocytes is pH dependent. Chondrocytes were labeled with uranyl acetate at pH 3.1 (a), 3.5 (b), 4.3 (c), 5.0 (d), with uranyl acetate oxalate at pH 7.0 (e), or with osmium tetroxide (f). Cells labeled with uranyl acetate at pH 3.1 or 4.3 (a and c) were weakly labeled, whereas at pH 3.5 the labeling was strong (b). At pH 5.0 uranyl acetate stained the gel but precipitated inside the fixed gel (d, arrows). No staining of the gel was detected when cells were stained with uranyl acetate oxalate at pH 7.0 (e), or with osmium tetroxide (f).

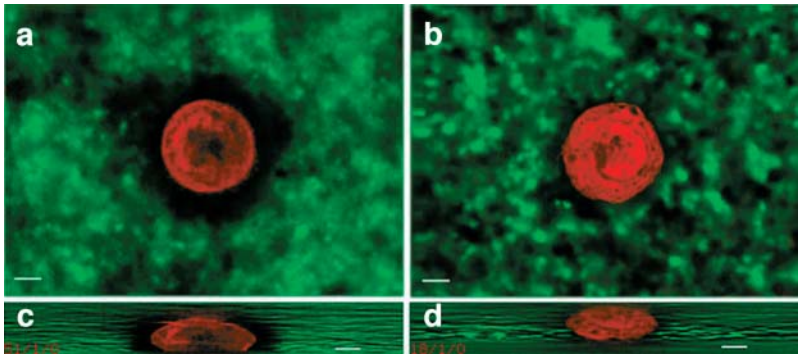


FIGURE 4 3D reconstruction of the pericellular hyaluronan coat by particle exclusion assay. (a and b) Fluorescence micrographs of rhodamine-labeled chondrocytes immersed in medium containing FITC-labeled silica beads. Cells were allowed to adhere to glass coverslips for 25 min before fixation, and labeled with tetramethyl rhodamine isothiocyanate (red). They were then incubated with FITC-labeled 0.4- μm silica beads (green). Micrographs were taken with a digital microscope (DeltaVision) able to generate 3D images by image reconstruction from a series of z-sections at 0.5- μm resolution. The excluded volume is dark. Untreated cells have 5- to 6- μm wide excluded zone around them (a), whereas beads reach up to the surface of hyaluronidase treated cells (b). (c and d)

Deconvoluted and reconstituted images along the z axes. Untreated cells (c) have a 1.2- μm excluded zone also on the apical region, whereas hyaluronidase-treated cells (d) have no excluded volume. We note that imaging from oil into water reduces the height of the sample by a factor equal to the ratio of refractive index between oil and water. In addition, imaging with an oil objective deep into a water sample introduces depth dependent aberration. This, for 10 μm depth, may reach up to at least half the resolution of the objective (Kam et al., 1997). Everything considered, the excluded volume in the apical region may reach up to \sim 2- μm thickness. The beads appear as segments because of Brownian motion. Scale bar, 5 μm .

flow shows that \sim 80% of the cells remained firmly attached. In contrast, hyaluronidase-treated cells, lacking the hyaluronan coat, did not bind to the surface, and were thus instantly removed by the flow (Fig. 5, compare a to b and Movie 2 b, Supplementary Material). Only \sim 1.5% of the hyaluronidase-treated cells remained attached. We conclude that the early stages of chondrocyte adhesion are hyaluronan mediated.

Given the thickness of the hyaluronan coat surrounding cells such as chondrocytes, it is conceivable that the first interactions between the cells and the matrix are mediated by a relatively soft and viscous gel. To determine the mechanical properties of this adhesion, cells were exposed to a constant flow 25 min after seeding, and their forced translocation was recorded by time-lapse phase microscopy at 30 images/min. Examination of these movies showed that many of the attached untreated cells passively drifted in the general direction of flow before detaching from the surface. Tracking of the moving cells pointed to an average translocation of $55.5 \pm 31.6 \mu\text{m}$ (range: 20.1–130.3 μm), at an average speed of $2.3 \pm 1.6 \mu\text{m}/\text{sec}$ (range: 0.7–3.9 $\mu\text{m}/\text{sec}$). Individual “translocation tracks” can be visualized by comparing images taken at different time points, as in Fig. 5 d' and d' + 1'. Both are magnifications of the marked area in Fig. 5 d taken at a 60-s interval. In Fig. 5 d' + 1' the pathway of each cell was reconstructed from the 30 time-lapse images in between. This behavior of passive translocation under flow is most probably due to rolling or sliding of the cells on a hyaluronan “cushion,” as the distance covered is too large to be associated with cells anchored through integrin-mediated adhesions.

Considering its thickness, it is conceivable that the pericellular coat of chondrocytes comprises a multiple layer of entangled hyaluronan molecules. It is thus possible that cells, passively translocating under flow, will leave behind surface-bound hyaluronan footprints. To examine such possibility, chondrocytes were subjected to flow as described above, then fixed and incubated with biotinylated hyaluronan binding proteins (bHABP), followed by streptavidin-CY3.

Fluorescence microscopy examination of these specimens revealed tracks of hyaluronan, generally located upstream to the cells (Fig. 6). Additional patches of hyaluronan were scattered on the surface, probably marking sites where cells had drifted and detached (data not shown). The average length of these hyaluronan “footprints” was $71.8 \pm 21.3 \mu\text{m}$ (ranging from 28 to 105 μm). The larger “footprints” were left by groups of more than one cell, thus the “footprints” correspond in their size to the drifting distance of cells under flow. In contrast to untreated cells, hyaluronidase-treated cells readily detach, and do not drift when subjected to flow.

A6 cells were subjected to the same procedure described above for chondrocytes, except that the time of incubation before application of flow was reduced to 5 min. Upon application of flow, \sim 80% of the cells remain attached to the glass. In contrast to chondrocytes, these cells do not drift but occasionally vibrate around their attachment centers with maximal dislocations of the order of μm . Even upon application of maximal flow rate, equivalent to a force of 61.8 dynes/cm², essentially all the cells remained anchored to the glass. Posttreatment of the glass with hyaluronan binding protein does not reveal any traces of hyaluronan. After hyaluronidase treatment, <45% of the cells remain attached to the glass, confirming that their attachment is hyaluronan mediated.

The behavior of A6 cells indicates that the hyaluronan coat is not displaceable by application of shear force. Alternatively, these cells may rapidly switch from hyaluronan-mediated adhesion to receptor-mediated attachment. We consider the possibility that in A6 cells single hyaluronan molecules span the whole thickness of the coat as a brush emanating directly from attachment sites on the membrane.

DISCUSSION

In this study we have addressed the involvement of the pericellular hyaluronan coat in the adhesion of cells to

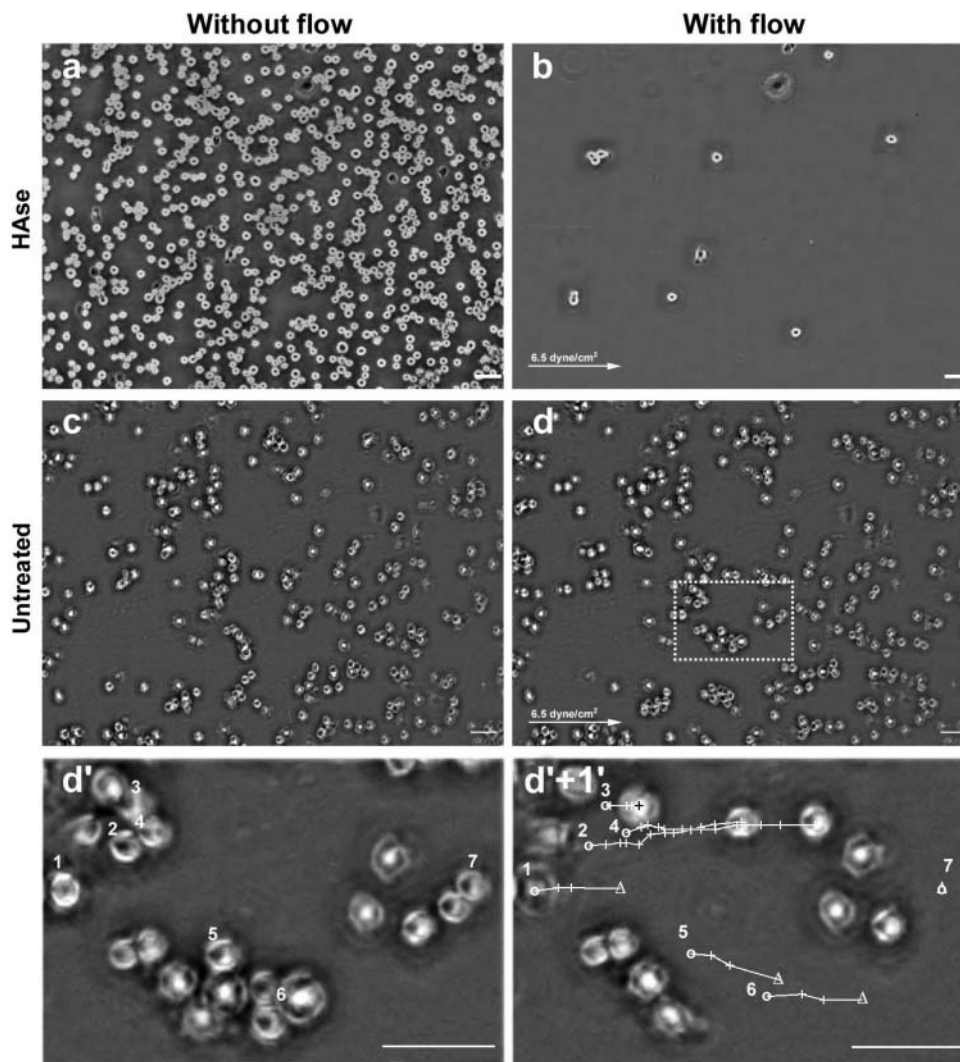


FIGURE 5 Hyaluronan-mediated adhesion: the role of hyaluronan in early adhesion and its resistance to shear stress. Chondrocytes (RCJ-P) were allowed to adhere to serum-coated glass for 25 min, then washed with a continuous flow of medium which exerted shear force of 6.5 dyne/cm^2 . Cell movement was recorded by a time-lapse phase microscope. (*a* and *c*) Cells before applying flow; (*b* and *d*) cells 2 s within the flow. (*a* and *b*) Hyaluronidase treated cells. (*c*) and (*d*) Untreated cells. The arrows indicate the flow direction. Hyaluronidase-treated cells washed away immediately after applying the flow (compare *a* to *b*). In contrast, untreated cells remained attached to the surface (compare *c* to *d*) and moved $43.10 \pm 10.79 \mu\text{m}$ before detaching from the surface. (*d'*) Enlargement of the area marked with a dashed line in *d*. (*d' + 1'*) The same frame as in *d'*, 60 s later. The circles mark the original position of seven selected cells; the crosses mark the cell position at 4-s intervals; the triangles mark the detachment position; the lines mark the cell paths. Cells 1, 5, and 6 moved $37.57\text{--}41.71 \mu\text{m}$ at the speed of $3.13\text{--}3.48 \mu\text{m/s}$ before detaching from the surface. Cells 2 and 4 traveled longer ($66.12\text{--}82.10 \mu\text{m}$) but slower ($1.10\text{--}1.47 \mu\text{m/s}$) and did not detach within 60 s of flow. Cell 3 started to move only 36 s after applying the flow, covering $13.46 \mu\text{m}$, and remained attached to the surface. Cell 7 did not move but detached 2 s after applying flow. Scale bar, $50 \mu\text{m}$.

external surfaces. Hyaluronan and its receptors, primarily CD44, are involved in many cellular processes, among them cell adhesion, motility, proliferation, and signaling (Borland et al., 1998; Toole, 2001). However, unlike the “conventional” ligand-receptor setting, many cells, such as chondrocytes, are surrounded by a thick hyaluronan layer whose properties, as well as its mode of interaction with the plasma membrane, can affect the adhesive process (McBride and Bard, 1979; Lee et al., 1993; Evanko et al., 1999). The first objective of the present study was to visualize and to determine the physical properties of the cell-associated hyaluronan. Performing ESEM on uranyl acetate stained cells, we have visualized a well defined, homogeneous, $4.4 \pm 0.7\text{-}\mu\text{m}$ -thick, hydrated, hyaluronidase-sensitive coat around chondrocytes (RCJ-P) in suspension and a $2.2 \pm 0.4\text{-}\mu\text{m}$ -thick coat around epithelial cells (A6).

Our results support the notion that hyaluronan surrounds both chondrocytes and epithelial cells as a gel phase, the exact concentration of which is yet to be determined. Although the external borders of the hyaluronan gel

surrounding individual cells are sharply defined, the coats of cells grouped together merge, forming one uniform layer around and between them (Fig. 3). The pericellular coat appears to be homogeneous and partially transparent to electrons, with sharp and defined borders, whereas the cell membrane appears blurred (Fig. 1). These features are interpretable within the framework of the experimental technique used. The hyaluronan coat becomes visible when the liquid water around the cells is gradually removed by evaporation. If single hyaluronan molecules sprout sparsely from the gel layer at its boundary, the water surface tension will force them to condense at the interface upon evaporation. As a result, hyaluronan coat borders appear sharp.

The image in wet-mode ESEM is acquired with a gas (GSE) detector, which exploits the water molecules saturating the microscope chamber to amplify the signal of the secondary electrons emitted by the sample. In our experimental set up, the uranyl ions introduced in the pericellular coat are used as particularly efficient stimulation

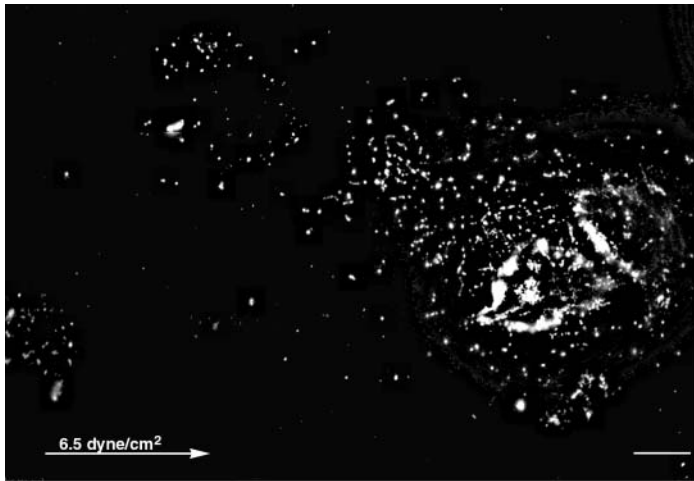


FIGURE 6 Hyaluronan “footprints” of chondrocytes are left after application of shear stress. Chondrocytes were treated with flow as described in Fig. 5, then fixed and incubated with biotinylated hyaluronan binding proteins followed by incubation with streptavidin-CY3. Tracks of hyaluronan are visible upstream to the cells. Cell with hyaluronan “footprints” of 75 μm . The arrow marks the flow direction. Scale bar, 10 μm .

of secondary electron emission. As the secondary electron emission is amplified in the pericellular coat, the emission due to the electrons back scattered from the membrane will be also amplified. This will result in a blurred image. In agreement with this interpretation, when the pericellular coat is removed, or in the absence of uranyl acetate treatment, a sharp image of the cell border is obtained (Fig. 1, *c* and *d*).

In agreement with the polyelectrolyte properties of the hyaluronan gel, the thickness of the pericellular coat is sensitive to pH (Fig. 2). Surprisingly, at pH 4.3 the hyaluronan coat appeared thinner and less intense than at pH 3.5. Many variables could be affected by the pH and result in reduction of the coat apparent density and size. One such variable is the uranyl ion solubility, which may affect its ability to bind hyaluronan at higher pH. We can furthermore envisage that at higher pH hyaluronan chains may be less entangled because of repulsion between like charges. Hyaluronan molecules that are not directly bound to the membrane receptors may consequently be washed away during sample preparation resulting in a thinner and less dense coat. This suggestion is supported by the proven trail of hyaluronan shed by the cells drifting in a flow, after contact with the substrate has been established.

Finally, in the particle exclusion assay the 0.4- μm silica beads do not penetrate the hyaluronan layer, and the pericellular coat is stable enough to form a few μm -thick layer in the vertical dimension (Fig. 4). We note here that, as hyaluronan is not likely to be affected by glutaraldehyde fixation, cross-linking of hyaluronan-bound proteoglycans (Lee et al., 1993; Evanko et al., 1999; Knudson and Knudson, 2001; Kiani et al., 2002) may contribute to the rigidity of the fixed coat.

All the above evidence is consistent with the pericellular coat being in a gel phase. It is mandatory at this point, to compare the results obtained here with what is known about the physical properties and structure of hyaluronan *in vitro* and in the extracellular matrix. Hyaluronan forms three-dimensional hydrated gels *in vitro*. The thickness of surface-

grafted hyaluronan as measured by imaging ellipsometry under humid atmosphere (Mathe et al., 1999) is within the range of 100 nm, which corresponds to 200-nm radius of gyration (Laurent, 1987). As expected from polyelectrolyte gels, the layer thickness is sensitive to salt concentration (Albersdorfer and Sackmann, 1999).

The hyaluronan polymer usually consists of 2000–20,000 disaccharides, with a molecular weight range of several million Daltons, depending on the tissue source (Toole, 2001). Concentrated (1 mg/ml) hyaluronan solutions form networks when carefully dried on mica or graphite (Jacoboni et al., 1999). Diluted solutions (1–5 $\mu\text{g}/\text{ml}$) of hyaluronan molecules of 4.2×10^6 Da, visualized with the atomic force microscope, showed separated hairpin-shaped molecules with a typical length of 6–7 μm (Cowman et al., 1998). High molecular weight hyaluronan was suggested to form a three-dimensional network of antiparallel hyaluronan ribbons, stabilized by specific hydrogen bonds between acetamido NH moieties and carboxylate groups on neighboring chains, and by hydrophobic interactions between the sugar aliphatic moieties (CH) (Hadler et al., 1982; Scott, 1992; Scott and Heatley, 1999, 2002). These interactions are proposed to be responsible for the gel-like characteristics of hyaluronan. The pericellular coat of eukaryotic cells contains, besides hyaluronan, also other proteins, among them proteoglycans such as aggrecan (Lee et al., 1993; Knudson and Knudson, 2001; Kiani et al., 2002) and versican (Evanko et al., 1999), which interact with hyaluronan. These can cross-link neighboring hyaluronan molecules, contributing to the stability of the hyaluronan-based gels around cells. The hyaluronan viscoelastic properties are extremely affected by the presence of those proteoglycans. Hyaluronan solutions from bacterial sources, which lack the hyaluronan binding proteoglycans, are viscoelastic liquids with a concentration-dependent viscosity typical of polyelectrolytes with excess salt rather than of gels (Gribbon et al., 2000; Krause et al., 2001).

The thickness of the hyaluronan layer observed around chondrocytes in this study is much larger than the expected molecular radius of gyration. It is thus conceivable that extended hyaluronan molecules anchored to membrane receptors project out from the membrane, forming thick brushes, when supported by a high density of receptors on the membrane. We note that the observed thickness is a moderate estimate, as hyaluronan layers progressively shrink with decreasing environment humidity (Mathe et al., 1999). We are currently testing the dimensions of the hyaluronan gel in cells completely immersed in water, using a novel approach (Thiberge et al., 2002).

The physical properties of the pericellular hyaluronan coat have a major impact on the interaction of cells with external surfaces. Due to its thickness, which is several orders of magnitude above the size of typical membrane proteins, the pericellular coat is most likely the first cellular component that encounters the matrix during the attachment process (Zimmerman et al., 2002). The properties of hyaluronan-mediated adhesion are thus strongly affected by the coat properties. Under shear stress of 6.5 dyne/cm² chondrocytes drifted on the matrix leaving trails of hyaluronan “foot-prints” (Fig. 6). Thus the thick chondrocyte pericellular coat can be stretched and peeled off the cell, at least in part. Assuming that the hyaluronan chains are not pulled off the receptor by these forces, this is consistent with the hyaluronan molecules being entangled in multiple layers. In contrast to chondrocytes, A6 cells, under a similar shear stress, remained anchored to the matrix. Their motions are limited to vibrations and oscillations around a fixed site, suggesting the model of suspended spheres anchored to the substrate through a mesh of long tethers. This behavior is consistent with hyaluronan molecules being attached to A6 cells in a “brush” configuration, where each hyaluronan molecule is directly attached to a receptor in the membrane.

The early, hyaluronan-mediated adhesion sets the stage for the establishment of receptor-mediated interactions between members of the integrin family and corresponding ECM proteins such as fibronectin or vitronectin (Geiger et al., 2001; Martin et al., 2002). There are various possible scenarios for this transition: Cells can extend long dynamic membrane projections (e.g., filopodia) that may protrude beyond the hyaluronan coat, forming a direct membrane contact. Chondrocytes, for example, contain microvilli, ranging in length from 1.14 to 2.84 μm (mean length: $1.76 \pm 0.49 \mu\text{m}$), based on transmission electron microscope and SEM measurements (data not shown). The chondrocyte hyaluronan coat is within the range of 3–5.6 μm (average $4.4 \pm 0.7 \mu\text{m}$, from ESEM measurements). The coat thickness was measured on chondrocytes that underwent fixation while in suspension. Considering the surface properties and the contribution to the pericellular coat rigidity of hyaluronan-bound proteoglycan cross-linking, we can assume that the measured coat dimensions are representative of those in live chondrocytes. The microvilli are thus hidden within the

hyaluronan coat; the latter may shrink upon interaction with the matrix, exposing the microvilli, ready to interact with the matrix and promote integrin-mediated adhesion. It is noteworthy that the microvilli were not detectable in the wet ESEM, suggesting that they either do not protrude beyond the border of the gel, or collapse during the observation.

An alternative scenario for the transition between hyaluronan-mediated and integrin-mediated adhesion is that the hyaluronan coat may be locally removed, exposing the integrins to the matrix. Removal of the hyaluronan coat could be achieved by lateral diffusion of hyaluronan receptors, by local degradation, by internalization of hyaluronan via the CD44 receptor (Knudson et al., 2002), or by local change of pH or ion concentration, which may lead to hyaluronan shrinkage (Albersdorfer and Sackmann, 1999).

Being hydrated, the pericellular coat provides a stable osmotic environment, thus buffering small instabilities. When chondrocytes were dried in the ESEM chamber by reducing the vapor pressure, the pericellular coat responded to the reduction in pressure with a delay of 10–15 min, whereas water droplets disappeared almost instantaneously. This is reminiscent of the behavior of hyaluronan in cartilage, synovial fluid, and the extracellular matrix, where it has the role of preserving tissue hydration and swelling by maintaining the osmotic pressure (Israelachvili and Wennerstrom, 1996; Knudson and Knudson, 2001; Toole, 2001).

Finally, the concept of cells being surrounded by a several- μm -thick pericellular coat with the properties of a gel is not to be considered lightly. It implies that every interaction with the environment around the cells, soluble or insoluble, will be affected by the presence of such layer that any component, be it signaling molecules, proteolytic enzymes, metabolites, nutrients, or drugs, need to penetrate to reach the cell membrane.

SUPPLEMENTARY MATERIAL

An online supplement to this article can be found by visiting BJ Online at <http://www.biophysj.org>.

We thank Prof. S. Margel (Bar Ilan University, Ramat Gan, Israel) for providing us with FITC-labeled silica beads. L.A. is an incumbent of the Dorothy and Patrick Gorman Professorial Chair. B.G. is an incumbent of the E. Neter Chair in Tumor and Cell Biology.

This work was supported by a grant from the Ziegler family trust.

REFERENCES

- Adams, J. C. 2001. Cell-matrix contact structures. *Cell. Mol. Life Sci.* 58:371–392.
- Albersdorfer, A., and E. Sackmann. 1999. Swelling behavior and viscoelasticity of ultrathin grafted hyaluronic acid films. *Eur. Phys. J. B.* 10:663–672.
- Bajorath, J. 2000. Molecular organization, structural features, and ligand binding characteristics of CD44, a highly variable cell surface glycoprotein with multiple functions. *Proteins.* 39:103–111.

- Bard, J. B., W. H. McBride, and A. R. Ross. 1983. Morphology of hyaluronidase-sensitive cell coats as seen in the SEM after freeze-drying. *J. Cell Sci.* 62:371–383.
- Borland, G., J. A. Ross, and K. Guy. 1998. Forms and functions of CD44. *Immunology.* 93:139–148.
- Cowman, M. K., M. Li, and E. A. Balazs. 1998. Tapping mode atomic force microscopy of hyaluronan: extended and intramolecularly interacting chains. *Biophys. J.* 75:2030–2037.
- Danilatos, G. D. 1991. Review and outline of environmental SEM at present. *J. Microsc.* 162:391–402.
- de Gennes, P. G. 1987. Polymers at the interface; a simplified view. *Adv. Colloid Interface Sci.* 27:189–209.
- Evanko, S. P., J. C. Angello, and T. N. Wight. 1999. Formation of hyaluronan- and versican-rich pericellular matrix is required for proliferation and migration of vascular smooth muscle cells. *Arterioscler. Thromb. Vasc. Biol.* 19:1004–1013.
- Geiger, B., A. Bershadsky, R. Pankov, and K. M. Yamada. 2001. Transmembrane crosstalk between the extracellular matrix–cytoskeleton crosstalk. *Nat. Rev. Mol. Cell Biol.* 2:793–805.
- Gibbon, P., B. C. Heng, and T. E. Hardingham. 2000. The analysis of intermolecular interactions in concentrated hyaluronan. *Biochem. J.* 350:329–335.
- Hadler, N. M., R. R. Dourmashkin, M. V. Nermut, and L. D. Williams. 1982. Ultrastructure of a hyaluronic acid matrix. *Proc. Natl. Acad. Sci. USA.* 79:307–309.
- Hanein, D., B. Geiger, and L. Addadi. 1994. Differential adhesion of cells to enantiomorphous crystal surfaces. *Science.* 263:1413–1416.
- Hanein, D., B. Geiger, and L. Addadi. 1995. Cell adhesion to crystal surfaces: a model for initial stages in the attachment of cells to solid substrates. *Cells and Materials.* 5:197–210.
- Hanein, D., H. Sabanay, L. Addadi, and B. Geiger. 1993. Selective interactions of cells with crystal surfaces. Implications for the mechanism of cell adhesion. *J. Cell Sci.* 104:275–288.
- Israelachvili, J., and H. Wennerstrom. 1996. Role of hydration and water structure in biological and colloidal interactions. *Nature.* 379:219–224.
- Jacoboni, I., U. Valdre, G. Mori, D. Quaglino, Jr., and I. Pasquali-Ronchetti. 1999. Hyaluronic acid by atomic force microscopy. *J. Struct. Biol.* 126:52–58.
- Kam, Z., D. A. Agard, and J. W. Sedat. 1997. Three-dimensional microscopy in thick biological samples: a fresh approach for adjusting focus and correcting spherical aberration. *Bioimaging.* 5:40–49.
- Kiani, C., L. Chen, Y. J. Wu, A. J. Yee, and B. B. Yang. 2002. Structure and function of aggrecan. *Cell Res.* 12:19–32.
- Knudson, C. B., and W. Knudson. 2001. Cartilage proteoglycans. *Semin. Cell Dev. Biol.* 12:69–78.
- Knudson, W., G. Chow, and C. B. Knudson. 2002. CD44-mediated uptake and degradation of hyaluronan. *Matrix Biol.* 21:15–23.
- Krause, W. E., E. G. Bellomo, and R. H. Colby. 2001. Rheology of sodium hyaluronate under physiological conditions. *Biomacromolecules.* 2:65–69.
- Laurent, T. C. 1987. Biochemistry of hyaluronan. *Acta Otolaryngol. Suppl.* 442:7–24.
- Lee, G. M., B. Johnstone, K. Jacobson, and B. Caterson. 1993. The dynamic structure of the pericellular matrix on living cells. *J. Cell Biol.* 123:1899–1907.
- Lee, J. Y., and A. P. Spicer. 2000. Hyaluronan: a multifunctional, mega Dalton, stealth molecule. *Curr. Opin. Cell Biol.* 12:581–586.
- Martin, K. H., J. K. Slack, S. A. Boerner, C. C. Martin, and J. T. Parsons. 2002. Integrin connections map: to infinity and beyond. *Science.* 296:1652–1653.
- Mathe, G., A. Albersdorfer, K. R. Neumaier, and E. Sackmann. 1999. Disjoining pressure and swelling dynamics of thin adsorbed polymer films under controlled hydration conditions. *Langmuir.* 15:8726–8735.
- McBride, W. H., and J. B. Bard. 1979. Hyaluronidase-sensitive halos around adherent cells. Their role in blocking lymphocyte-mediated cytotoxicity. *J. Exp. Med.* 149:507–515.
- Scott, J. E. 1992. Supramolecular organization of extracellular matrix glycosaminoglycans, in vitro and in the tissues. *FASEB J.* 6:2639–2645.
- Scott, J. E., and F. Heatley. 1999. Hyaluronan forms specific stable tertiary structures in aqueous solution: a ¹³C NMR study. *Proc. Natl. Acad. Sci. USA.* 96:4850–4855.
- Scott, J. E., and F. Heatley. 2002. Biological properties of hyaluronan in aqueous solution are controlled and sequestered by reversible tertiary structures, defined by NMR spectroscopy. *Biomacromolecules.* 3:547–553.
- Tadmor, R., N. Chen, and J. Israelachvili. 2002. Thin film rheology and lubricity of hyaluronic acid solution at a normal physiological concentration. *J. Biomed. Mater. Res.* 61:514–523.
- Thiberge, S., E. Moses, and O. Zik. 2002. Electron microscopy of cells in a wet environment: A new high resolution imaging technique. *Biophys. J.* 82:495a.
- Toole, B. P. 2001. Hyaluronan in morphogenesis. *Semin. Cell Dev. Biol.* 12:79–87.
- Weigel, P. H., V. C. Hascall, and M. Tammi. 1997. Hyaluronan synthases. *J. Biol. Chem.* 272:13997–14000.
- Zamir, E., B. Z. Katz, S. Aota, K. M. Yamada, B. Geiger, and Z. Kam. 1999. Molecular diversity of cell-matrix adhesions. *J. Cell Sci.* 112:1655–1669.
- Zimmerman, E., B. Geiger, and L. Addadi. 2002. Initial stages of cell-matrix adhesion can be mediated and modulated by cell-surface hyaluronan. *Biophys. J.* 82:1848–1857.